IN-ORBIT CALIBRATION OF VIGNETTING IN EPIC

D.H. Lumb[1]

ESA Payload Technology Division, Research and Scientific Support Department, ESTEC, Postbus 299, NL-2200 AG Noordwijk, The Netherlands

Abstract

We briefly describe the in orbit measurements of the mirror vignetting, using observations of SNR G21.5-09. The instrument features which complicate these measurements are briefly described, and we show the spatial and energy dependences, outlining assumptions made in deriving the eventual agreement between theory and measurement

Key words: Missions: XMM-Newton

1. Introduction

The reduction in effective area with radial distance from the field of view centre, or vignetting, must be accurately determined to support a number of important science investigations:

- Extended targets (e.g. clusters) whose radial brightness distribution must be accurately traced in order to determine mass
- Population studies - where exposure maps and counts to flux conversions depend upon vignetting correction
- Background studies of diffuse cosmic radiation where the normalisation for integrated flux over large areas of sky must be determined

Direct measurement on-ground was prevented because all X-ray beam measurements were performed in a non-parallel beam. The installation of an X-ray stray-light baffle and the RGA stack introduced potential complications that could only be followed in the visible light at the EUV parallel beam facility, so that X-ray energy dependence was not measureable. Although the measured geometric vignetting factor was comparable with predictions, it was necessary to use in-orbit data to confirm the energy dependence, and further check that the geometric factor was maintained through the spacecraft AIV and launch campaigns.

In essence, to measure the vignetting we need to measure a compact, simple spectrum non-variable source at locations off-axis, and compare the inferred spectrum with that of the same object measured on-axis. Truly point sources with reasonable brightness are precluded because the effects of pile-up are severe, and furthermore vary with the off-axis PSF changes, as well as the count rate reduction due to the vignetting itself. Extended objects require a complex ray-tracing and PSF-folding to account properly for the vignetting component. While a number of viable targets were selected for the in-orbit calibration, we have concentrated on G21.5-09 for this work (see also Warwick et al 2001):

- It is moderately compact (core slightly larger than the PSF FWHM but $\leq$1 arcmin)
- Absorbed simple power law spectrum
- Count rate just below the on-axis pile-up limit

2. Observation Set up

The initial choice of pointing locations was complicated by the need to ensure that no significant portion of the remnant fell near CCD gaps. Given the orthogonal orientation of the two MOS cameras, together with the totally different gap patterns in the PN, this severely constrained the orientation avaialable, and an angle $\sim$7 degrees off the nominal chip axes, and a field angle of 10 arcminutes was chosen.

As a consequence of the grating array angles and blocking fraction, the vignetting in the MOS cameras is expected to be a strong function of azimuthal angle, so 4 locations were scheduled to sample the extreme ranges of RGA blocking. A detailed simulation of expected source parameters indicated that $\sim$30ks exposure per location was needed to measure the vignetting with adequate leverage to highest energies.

3. Initial Analysis

The observations were conducted in April 2000 during a period of extended proton flares. Not only did this curtail usable exposure duration to $\sim$5 – 20 ks per exposure, but even the quietest periods suffered higher than usual quiescent background. Therefore considerable effort was expended on understanding the effects of background subtraction using in-field areas close to the target.

Our understanding of the MOS azimuthal variations in vignetting were undermined by significant variations ($\sim$10%) in relative vignetting measured in the PN camera, from azimuth to azimuth. This was attributed to a combination of incomplete background correction and to

Proc. Symposium *'New Visions of the X-ray Universe in the XMM-Newton and Chandra Era'* 26–30 November 2001,

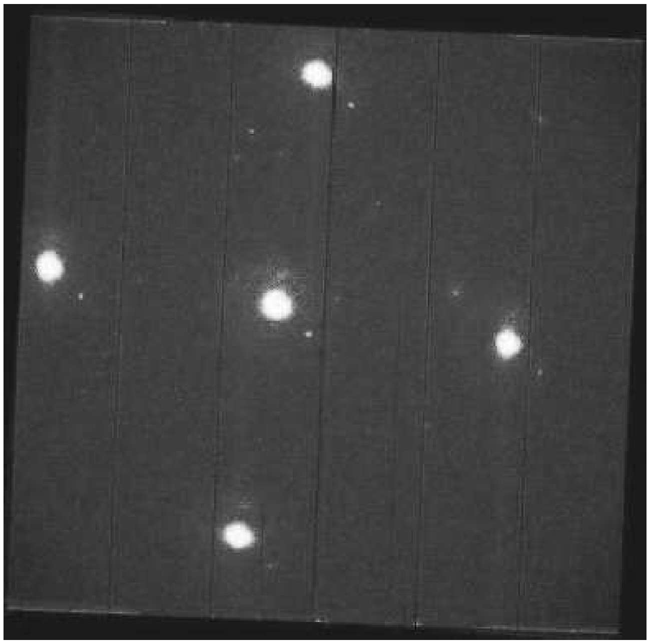

Figure 1. Merged image of the 5 major pointings made on G21.5-09

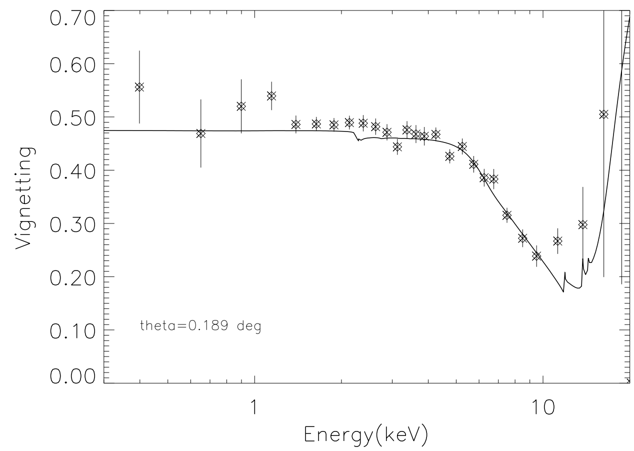

Figure 2. Relative *vignetting of the PN telescope for an off-axis angle of11.3 arcminutes, compared with the nominal boresight location*

discrepancies in the exposure calculations influenced by the higher than nominal background.

Eventually it was realised that these relative variations were correlated with camera orientations, and traced back to similar unresolved discrepancies between mirror alignment lens and inferred telescope axes measured at the EUV test facility (Stockman et al 1997). At the time these oientation discrepancies were claimed to be irreproducible to ~ 20 arcsec level, but were also seen in similar magnitude and direction in the Panter calibration of maximum throughput orientation (Egger et al 1997).

For the in-orbit data, acceptable agreement between predictions and inferred vignetting value could be obtained by positing an offset between the nominal telescope axis intersection at the focal plane, and the actual location of *both* the nomainal telescope axis and the boresight axis of the XMM system which determines the location of the central target.

Under the assumption of azimuthal symmetry (although this is not necessarily valid due to the mechanical tolerances on mounting the X-ray baffle), we compare the counts per energy bin between *pseudo* on- and off-axis locations as measured on G21.5-09, and the relative vignetting between the corresponding locations. The energy bins' widths were varied semi-logarithmically to maintain reasonable signal:noise per bin.

4. Results

A single azimuth vignetting measurement for the PN camera, in the lowest background exposure, is shown in Figure 2. The energy at which the vignetting decreases strongly is determined by the critical angle for grazing incidence at the off-axis angle of the target (11 arcminutes in this case). The increase again at higher energies is a consequence of only the innermost mirror shells providing substantial reflectivity. For a small diameter shell, at high energies, the area increases intially with off-axis angle: on one side of the mirror the parabola grazing angle is shallower than for the on-axis geometry. The corresponding hyperbola graze angle is then larger but because of the asymmetry of the reflectance vs. angle curve the higher reflectivity on the parabola dominates the product of the reflectances. A subsequent calibration set in ca. April 2001 at larger off-axis angle allowed some measure of sensitivity to the change in θ, and confirms the validity of the model.

A comparable vignetting measurement for the MOS cameras is shown in Figure 3. Due to the lower effective area of the MOS cameras, the S:N is lower than the PN camera, and the energy bins are wider. It was found again that there was a potential telescope axis misalignment. However records of the tests in ground facility were not so clear, because the installation of the RGA had blocked the access to the mirror alignment lens for most tests. Relying purely on inferred alignment of the axis based on the vignetting itself undermines the goal of directly measuring the effect of RGA azimuthal blocking factor.

5. Energy Dependence

The PN data are relatively close in off-axis angle, and have no intrinsic azimuthal dependence, so we should be able to average the 4 separate locations to check the predicted energy dependence is correctly reproduced. This is shown in Fig. 4.

For the MOS data repeating the exercise is not really valid, given the large variation in RGA blocking with az-

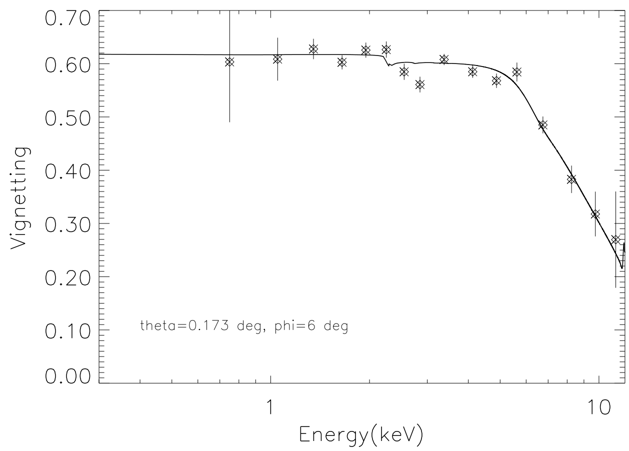

Figure 3. Relative *vignetting of the MOS1 telescope for an off-axis angle of 10.4 arcminutes, compared with the nominal boresight location*

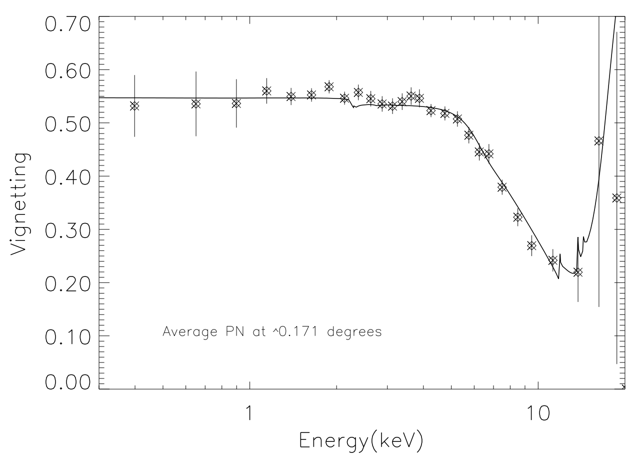

Figure 4. Relative *vignetting of the PN telescope after averaging all azimuths around 10.3 arcmins off-axis. The energy dependence is in good agreement*

imuth. However to discern if the placement of RGA gratings and ribs upsets the “grey” filter properties via. differential shadowing of some sub-sets of shells, we nevertheless form the same average response in the 2 MOS cases. There seems to be no significant energy dependent discrepancies.

6. Conclusions

The energy dependent vignetting calibration can be well matched to pre-launch predictions, but only on an assumption that the telescope optical axis is not well-alligned with the telescope boresight. This is not unexpected fol-

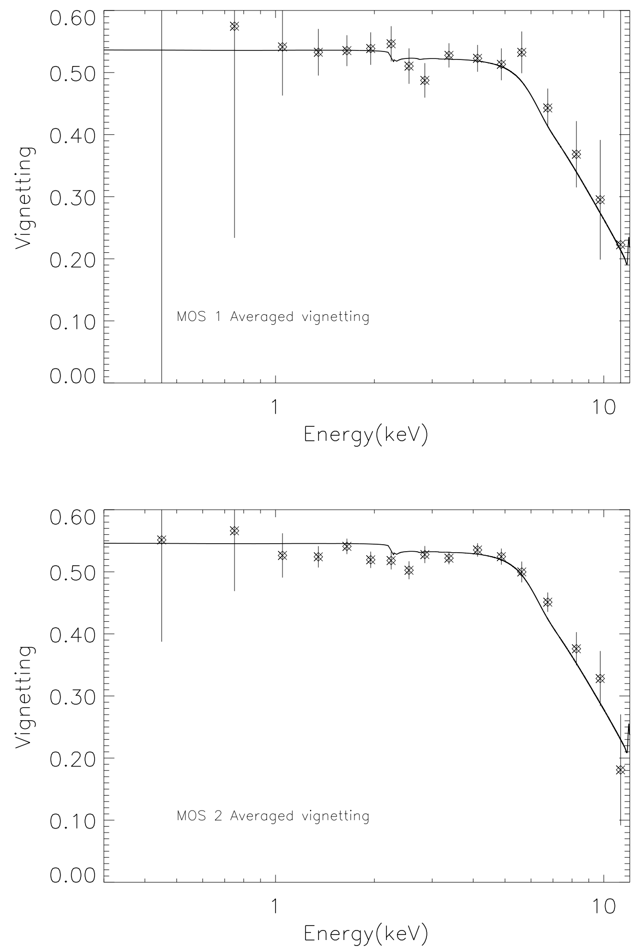

Figure 5. Relative *vignetting of the MOS telescopes after averaging all azimuths around 10.3 arcmins off-axis. The energy dependence is in good agreement*

lowing difficulties on-ground of maintaining and/or measuring the telescope axis to better than 10’s arcseonds.

We note finally that the assumed telescope axis misalignment implies that “on-axis” targets at the common boresight location are actually at a slightly different vignetting value per telescope. We speculate that this partly accounts for some of the observed flux discrepancies between the MOS and PN cameras.

7. Acknowledgements

Fruitful discussions with C Erd, P Gondoin, A Finoguenov and D Neumann are gratefully acknowledged

References

Egger, R., Aschenbach, B., Bräuninger et al 1997 Panter Test Reports XMM-TS-PA063/970829, XMM-TS-PA070/980115 etc.

Stockman, Y., Tock, J-P., Thome, M. et al 1997 CSL Test Reports, RP-CSL-MEV-97032, RP-CSL-MEV-97019 etc.

Warwick, R.S., Bernard, J-P., Bocchino, F. et al 1996, A&A 365 L248.